



BIOCHEMISTRY & MOLECULAR BIOLOGY *Letters*

Full Paper

BCAMBL, 1(2), 2015 [065-073]

A new fluorescent probe for turn-on detection of pH using 2,6-bis-[(1-H-benzoimidazol-2-ylmethylimino)-methyl]-4-methylphenol: imaging application in living cells

Uday Chand Saha¹, Sushil Kumar Mandal², Siddhartha Pal¹, Anisur Rahman Khuda-Bukhsh², Pabitra Chattopadhyay¹, Koushik Dhara^{3,*}

¹Department of Chemistry, Burdwan University, Golapbug, Burdwan 713104, West Bengal, (INDIA)

²Cytogenetics and Molecular Biology Laboratory, Department of Zoology, University of Kalyani, Kalyani 741235, (INDIA)

³Department of Chemistry, Sambhu Nath College, Labpur, Birbhum 731303, West Bengal, (INDIA)

E-mail: dharachem@gmail.com

ABSTRACT

A newly designed, easy to make and simple molecule, 2,6-bis-[(1-H-benzoimidazol-2-ylmethylimino)-methyl]-4-methylphenol (HL¹) behaves as a highly pH-responsive selective fluorescent probe in a Britton-Robinson buffer at 25°C. The pH titration indicates that the fluorescence intensity increases more than 36-fold in the pH range of 5.0-8.5 with pK_a value of 6.99 (±0.09). This enhancement of fluorescence intensity with increase in pH is accounted by the formation of the phenoxide form, L¹, generated by the deprotonation of HL¹ in higher pH. The DFT calculations reveal that the energy difference between the HOMO-LUMO of L¹ is less than that of HL¹ and it is evidenced by the red shift observed in the UV-vis absorption studies experimentally. The presence of the biologically relevant ions i.e. Na⁺, K⁺, Ca²⁺ etc. and the other important metal ions e.g. Cr³⁺, Mn²⁺, Pb²⁺ etc. do not show any significant contribution in the fluorescence behavior. The fluorescent imaging of HeLa cells also demonstrates that the designed probe has great value in monitoring intracellular H⁺ within living cells as it has no significant cytotoxic effect.

© 2015 Trade Science Inc. - INDIA

KEYWORDS

Fluorescence probe;
Selective;
Ph;
Cellular imaging.

INTRODUCTION

In recent years, the design and synthesis of fluorescent probes integrated with a sensing function is an area of intense research. Synthetic fluorescent probes are powerful tools in cell biology for the nondestructive measurement of intracellular species

owing to their simplicity and sensitivity^{1,2}. Also, fluorescent probes have been employed in many areas of research such as medicine, industry and the environment due to the high sensitivity of fluorescence spectroscopy that allows the detection of very low concentration of the analyte³⁻⁶. Biochemical processes frequently involve protonation and

Full Paper

deprotonation of biomolecules with concomitant changes in the pH of the environment in many cellular events, such as cell growth^[7], calcium regulation^[8], endocytosis^[9], chemotaxis^[10], and other cellular processes. Cytoplasmic pH is strongly regulated by a complex interaction of H⁺-transport, H⁺-consuming and -producing reactions, and H⁺ buffering^[11,12]. Also the pH maintaining within the desired physiological range is very much essential for enzyme and ion channel activity, protein stability, and many other processes that are responsible for cell growth, development, and survival^[12].

Measurement of pH by the technique based on fluorescence is well established for both sensing and imaging applications. As minor variations of intracellular pH may induce cellular dysfunction, development of desirable pH fluorescent probes, having excitation profiles in the visible region, should be highly sensitive to the change of pH. In general, two types of fluorescent pH probes have been developed, i.e. probes for cytosol which work at a pH of about 6.8–7.4^[13–18], and probes for acidic organelles such as lysosomes and endosomes, which function in the pH range of about 4.5–6.0^[19–22]. A limited number of pH-responsive fluorescent probes has been developed to monitor diverse physiological and pathological processes^[23]. Limitations of the currently available pH probes include low sensitivity and/or excitation profiles in the ultraviolet region. Among the fluorescent pH probes that have been reported, only a small number are practical for intracellular imaging^[21,24–28].

To overcome these problems, we have designed and synthesized a new simple, easy to make, small probe, 2,6-bis-[(1-*H*-benzimidazol-2-yl)methylimino)-methyl]-4-methyl-phenol (HL¹) which behaves as a highly pH-responsive selective fluorescent receptor with a pK_a value 6.99 (±0.09) in a Britton-Robinson buffer at 25 °C. The probe shows more than 36-fold fluorescence enhancement when pH is shifted from 5.0 to 8.5. Also the protonation/deprotonation profile of HL¹ with the gradual change in pH was investigated by spectrophotometric titration in the same environmental condition. Interestingly, biologically relevant ions i.e. Na⁺, K⁺, Ca²⁺ etc. and the other metal ions e.g. Cr³⁺, Mn²⁺, Pb²⁺ etc.

do not interfere this fluorescence behavior. To the best of our knowledge, this type of small molecule as a new fluorescent probe for sensing biological pH for cellular imaging in living cells is still unexplored.

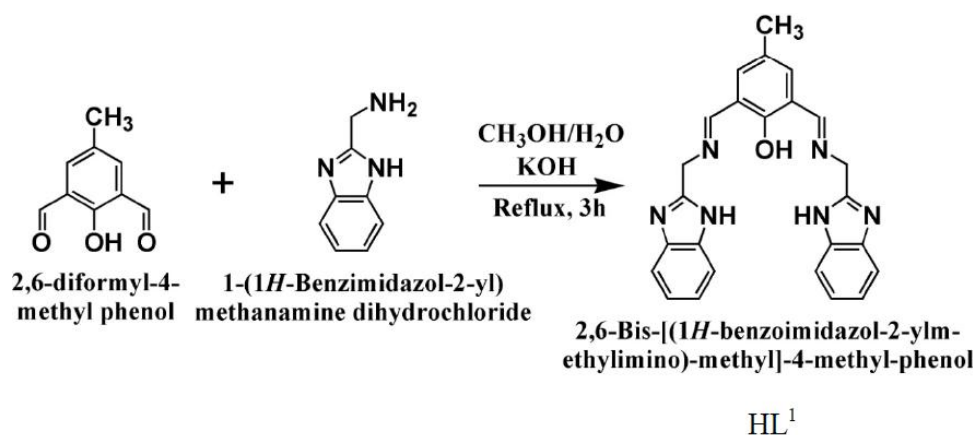
EXPERIMENTAL SECTION

Materials and physical measurements

All reagents and chemicals were purchased from Sigma and used without further purification. Solvents used for spectroscopic studies were purified and dried by standard procedures before use. FT-IR spectra were obtained on a JASCO FT-IR model 460 spectrometer using KBr disk. Elemental analysis was carried out on a Perkin Elmer model 2400 elemental analyzer. Fluorescence spectra and absorption spectra were performed using a HITACHI F-4500 Fluorescence Spectrophotometer and JASCO UV/VIS/NIR V-570 Spectrophotometer respectively. ESI mass spectra were recorded on a Qtof Micro YA263 mass spectrometer. ¹H and ¹³C NMR spectra were recorded on a Bruker AC300 spectrometer using TMS as an internal standard in D₆-DMSO solvents. The measurement of pH was carried out with the help of a digital pH meter (Systronics, Model 335).

Synthesis of 2,6-bis-[(1-*H*-benzimidazol-2-yl)methylimino)-methyl]-4-methyl-phenol (HL¹)

2,6-diformyl-4-methylphenol was synthesized starting from p-cresol following a published procedure^[29]. To a solution of 2,6-diformyl-4-methylphenol (0.164 g, 1.0 mmol) in methanol (30 mL) was added 1-(1-*H*-Benzimidazol-2-yl)methanamine dihydrochloride (0.220 g, 2.0 mmol) dissolved in methanol (10 mL) followed by the addition of 5 mL aqueous solution of KOH (0.123 g, 2.2 mmol) (Scheme 1). The reaction mixture was stirred first for 1 h and finally heated under refluxed condition for further 3.0 h. After completion of the reaction the solvent was evaporated in vacuum and 30.0 mL methanol was added to dissolve the crude compound and then it was filtered solution. The yellowish colored crystalline product (HL¹) was obtained by the slow evaporation of the filtered solution after few

Scheme 1 : Synthesis of HL¹

days in a good yield (Yield = 0.346 g, 82%). Elemental analysis (%): calcd for C₂₅H₂₂N₆O: C 71.07, H 5.25, N 19.89; Found: C 70.59, H 5.20, N 19.97; FT-IR (KBr phase) ($\nu_{\text{max}}/\text{cm}^{-1}$): $\nu_{\text{C=N}}$ 1668, $\nu_{\text{C-H}}$ 2958 $\nu_{\text{N-H}}$ 3178. ESI mass spectrum of HL¹ in water show peaks at $m/z = 423.1970$ and 445.0940 that can be assigned to the [M+H⁺] and [M+Na⁺] respectively where M = C₂₅H₂₂N₆O. ¹H NMR (DMSO-d₆, 300 MHz, δ ppm): 2.27 (s, 3H), 5.02 (s, 4H), and 6.72-7.81 (b, 12H); ¹³C NMR (DMSO-d₆, 100 MHz, δ ppm): 20.6, 56.1, 114.9, 122.2, 125.8, 130.5, 133.1, 141.2, 143.2, 151.3, 153.5.

General method of absorption and fluorescence analysis

HL¹ was dissolved in DMSO to obtain 10 mM stock solutions for both absorption and fluorometric titration study. Desired volume of DMSO stock was taken to dilute in Britton-Robinson buffer (1% DMSO) at 25 °C to reach the final concentration (10 μM) of the probe. Relative fluorescence quantum yields (Φ) were estimated by integrating the area under the fluorescence curves with the equation^[30]:

$$\Phi_{\text{sample}} = \Phi_{\text{standard}} \times \frac{\text{OD}_{\text{standard}} \times A_{\text{sample}} \times \eta_{\text{sample}}^2}{\text{OD}_{\text{sample}} \times A_{\text{standard}} \times \eta_{\text{standard}}^2}$$

where OD is optical density of the compound at the excitation wavelength, A is the area under the fluorescence spectral curve and η is the refractive index of the solvents. The standard used for the measurement of fluorescence quantum yield was tris(2,2'-bipyridyl) ruthenium(II) ($\Phi = 0.042$ in water, $\lambda_{\text{ex}} = 450 \text{ nm}$)^[31].

The investigation of fluorescence intensity

changes as a function of pH was analyzed by using Henderson-Hasselbalch equation^[32,33]: $-\log[(\text{FI}_{\text{max}} - \text{FI})/(\text{FI} - \text{FI}_{\text{min}})] = \text{pH} - \text{pK}_a$ where FI is the observed fluorescence intensity at a fixed wavelength, FI_{max} and FI_{min} indicate the corresponding fluorescence maximum and minimum intensities respectively.

Preparation of cell and in vitro cellular imaging with HL¹

Human cervical cancer cell, HeLa cell line was purchased from National Center for Cell Science (NCCS), Pune, India and was used throughout the study. Cell were cultured in Dulbecco's modified Eagle's medium (DMEM, Gibco BRL) supplemented with 10% FBS (Gibco BRL), and 1% antibiotic mixture containing penicillin, streptomycin and neomycin (PSN, Gibco BRL), at 37°C in a humidified incubator with 5% CO₂. For experimental study, cells were grown to 80-90% confluence, harvested with 0.025% trypsin (Gibco BRL) and 0.52 mM EDTA (Gibco BRL) in PBS (phosphate-buffered saline, Sigma Diagnostics) and plated at desired cell concentration and allowed to re-equilibrate for 24h before any treatment. Cells were rinsed with PBS and the extracellular pH was changed by the addition of 5 mM KOH or 50 mM HCl to DMEM, and the responses of intracellular pHs were monitored. The cells were incubated with the probe, HL¹ (10 μM) for 30 minutes at 25 °C at various pH i.e. 5.5, 6.0, 6.5 and 7.0. Then the cells were washed three times with the desired pH solution in DMEM. All experiments were conducted in DMEM containing 10% FBS and 1% PSN antibiotic. The imaging system

Full Paper

was composed of a fluorescence microscope (ZEISS Axioskop 2 plus) with an objective lens [10 \times].

Cell cytotoxicity assay

To test the cytotoxicity of HL¹, MTT [3-(4,5-dimethyl-thiazol-2-yl)-2,S-diphenyl tetrazolium bromide] assay was performed by the procedure described earlier^[34]. After treatments of the probe (5, 10, 20, 50, and 100 μ M), 10 μ l of MTT solution (10mg/ml PBS) was added in each well of a 96-well culture plate and incubated continuously at 25 $^{\circ}$ C for 6 h. All mediums were removed from wells and replaced with 100 μ L of acidic isopropanol. The intracellular formazan crystals (blue-violet) formed were solubilized with 0.04 N acidic isopropanol and the absorbance of the solution was measured at 595 nm with a microplate reader. Values are means \pm S.D. of three independent experiments. The cell cytotoxicity was calculated as percent cell cytotoxicity = 100% cell viability.

RESULTS AND DISCUSSIONS

Design and synthesis of HL¹

Design of the probe (HL¹) is one of the most important aspects in developing fluorescent probe for targeted analytes. HL¹ was synthesized by treating 2,6-diformyl-4-methylphenol with a derivative of benzimidazol methanamine in methanolic solu-

tion in presence of KOH. The structure of the probe indicates the simple Schiff-base formation with the amine and the aromatic aldehyde in a 2:1 ratio respectively. The probe is expected to act as a signal switcher through the phenolic hydroxyl group, which is envisioned to turn on when the target cation (H⁺) is bound.

Spectroscopic properties and optical responses to pH

We then examined the spectra properties of our probe. The fluorescence spectrum of HL¹ in Britton-Robinson buffer exhibits a very weak fluorescent with a maximum at 536 nm when excited at 425 nm at 25 $^{\circ}$ C in the low pH range. With the increase in pH the fluorescence intensity increases rapidly. The probe was almost non-fluorescent when H⁺ concentration falls to pH < 4.5. With decreasing H⁺ concentration to pH > 4.5, strong fluorescent appeared. Figure 1 shows the fluorescence emission spectra at different pH values. There is a more than 36-fold increase in the emission intensities ($\lambda_{\text{max}} = 536$ nm) within the pH range 5.0 - 8.5, which reveals the sensitivity of the pH probe.

Figure 2 shows the fluorescence emission changes at 536 nm with the pH titration curve of HL¹ (10 μ M) in Britton-Robinson buffer at 25 $^{\circ}$ C. The analysis of fluorescence intensity changes as a function of pH by using the Henderson-Hasselbalch

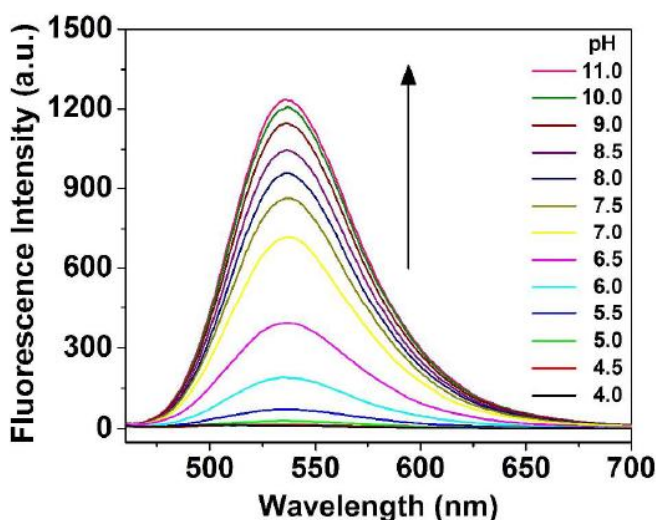


Figure 1 : Fluorescence spectra and pH titration curve of HL¹ (10 μ M) in Britton-Robinson buffer at 25 $^{\circ}$ C (λ_{ex} : 425 nm)

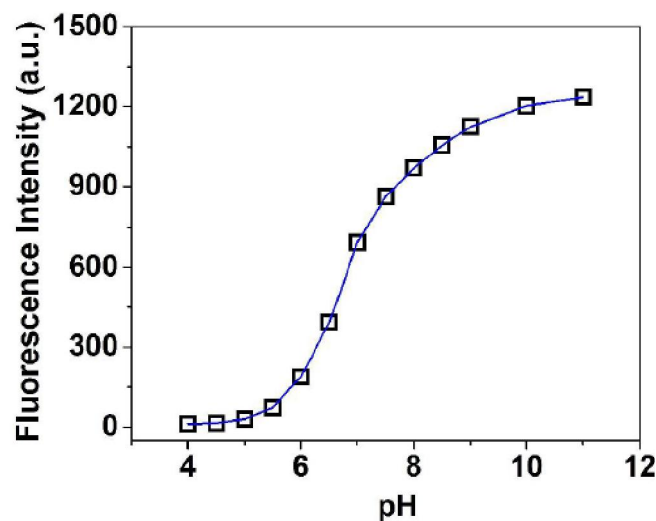


Figure 2 : The fluorescence emission changes at 536 nm with the pH titration curve of 10 μ M HL¹ in Britton-Robinson buffer at 25 $^{\circ}$ C (λ_{ex} : 425 nm)

equation^[32,33] yielded a pK_a of 6.99 (± 0.09), which is suitable for studying many of the biological organelles. The relative fluorescent quantum yield of the compound at the pH 5.0, 5.5, 6.0, 6.5 and 7.0 are 0.098, 0.148, 0.293, 0.354 and 0.463 respectively. In addition to that, an additional investigation of the probe was performed to determine the interferences of other ions because of the complexity of the intracellular environment in biological systems. To investigate this phenomenon, metal ion selectivity assays were performed while keeping the other experimental condition unchanged at pH 7.0. Fluorescence enhancement of HL^1 (10 μM) was not observed upon the addition of a large excess 100 equiv (1.0 mM) of biologically relevant metal ions, i.e., Na^+ , K^+ , and Ca^{2+} and 20 equiv of excess of several metal ions (Cr^{3+} , Mn^{2+} , Fe^{2+} , Fe^{3+} , Co^{2+} , Ni^{2+} , Cu^{2+} , Zn^{2+} , Cd^{2+} , Hg^{2+} and Pd^{2+}). In presence of 100 times (1 mM) excess of biologically significant ions i.e. Na^+ , K^+ together with HL^1 , almost no adverse effect on intensity was observed (Figure 3). Also in the case of relevant metal ion mixtures ($Fe^{3+} + Cu^{2+} + Zn^{2+}$) together with HL^1 , almost similar fluorescence enhancement was observed as shown by the free probe itself. Those results imply that HL^1 can selectively measure pH in the presence of various metal ions

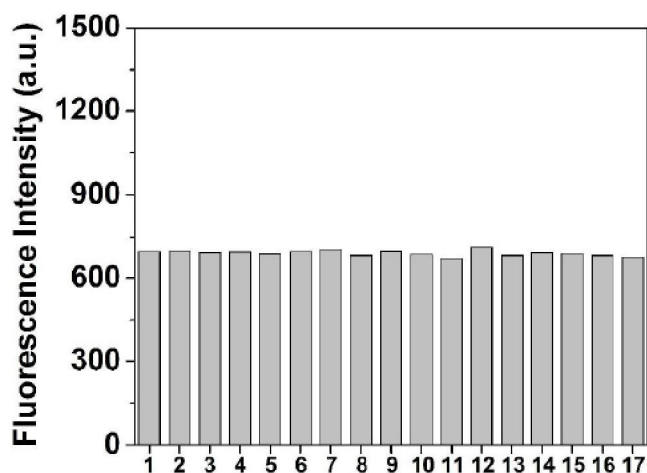
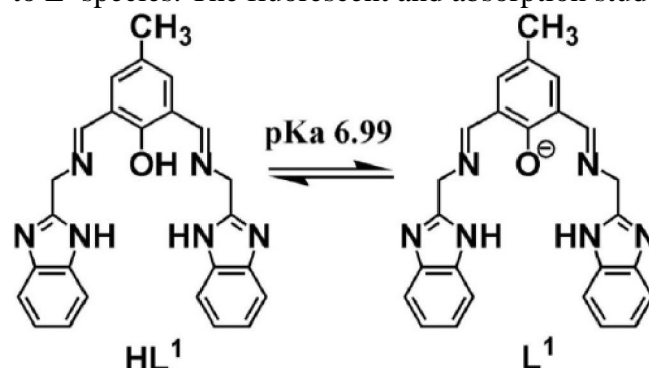


Figure 3 : The relative emission intensity change profile of the probe (HL^1) (10.0 μM) in the presence of various metal ions in Britton-Robinson buffer at 25 °C at pH 7.0 (λ_{ex} : 425 nm). [1-none, 2- Na^+ , 3- K^+ , 4- Ca^{2+} , 5- Cr^{3+} , 6- Mn^{2+} , 7- Fe^{2+} , 8- Fe^{3+} , 9- Co^{2+} , 10- Ni^{2+} , 11- Cu^{2+} , 12- Zn^{2+} , 13- Cd^{2+} , 14- Hg^{2+} , 15- Pd^{2+} , 16-($Na^+ + K^+$), 17-($Fe^{3+} + Cu^{2+} + Zn^{2+}$); Concentration of Na^+ , K^+ , Ca^{2+} were used as 1 mM and other metal ions were in 0.2 mM]

usually present in biological systems, and therefore, HL^1 might be considered as a selective fluorescent probe for pH sensing. It is also noteworthy that the effect of such metal ions on pH measurement is negligible, particularly when considering that the concentrations used for the experiment were significantly higher than those present in the intracellular environment.

This fluorescence increase with increase in pH is accounted by the formation of (phenoxide)^[35,36] of HL^1 in higher pH (Scheme 2). The mode of protonation/deprotonation of HL^1 with change in pH was studied by UV-vis spectrophotometric titration at 25 °C in Britton-Robinson buffer. Figure 4 demonstrated a characteristic UV-vis titration curve of HL^1 as a function of pH. The absorption intensity of the probe at 350 nm gradually decreased, accompanied by the formation of a new absorption peak at 422 nm, as the pH was increased stepwise from 5.0 to 9.0. Also there is a gradual increase in absorption intensities at 274 nm. The extinction coefficients (422 nm) of the compound are gradually enhanced to 0.07, 0.10, 0.13, 0.20, 0.26, 0.35, and $0.42 \times 10^4 M^{-1} cm^{-1}$ when pHs are increased to 5.06, 5.50, 6.01, 6.52, 7.01, 7.51, 8.05, and 9.0 respectively. The absorption maximum observed at 350 nm is attributed to the hydrogen-bonded phenolic form of HL^1 (L^1)^[35,36]. Intensity of the absorption band at 422 nm increases due to the formation of L^1 (phenoxide) with an increase in pH, i.e., the increase in extinction coefficient at 422 nm, with a concomitant appearance of isosbestic points at ca. 309 and 378 nm. These phenomena illustrated the transformation from free HL^1 to L^1 species. The fluorescent and absorption stud-



Scheme 2 : Formation of L^1 (Phenoxide) from HL^1 in higher pH

Full Paper

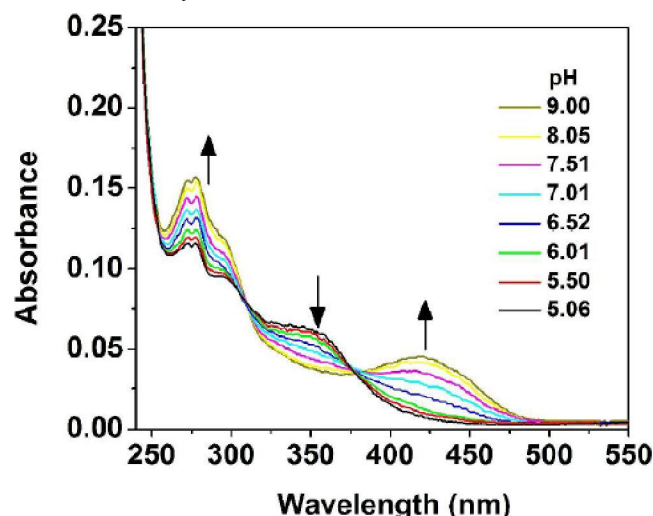


Figure 4 : UV-vis absorption of HL¹ (10 µM) to pH variation at 25 °C in britton-robinson buffer

5). The charge densities at the highest occupied molecular orbital (HOMO) of HL¹ resides on the benzimidazol unit, with no charge density on 2,6-bis-iminomethyl-4-methylphenol part. On the other hand, lowest unoccupied molecular orbital (LUMO) do not possess charge density on the benzimidazole molecule rather it is located at the 2,6-bis-iminomethyl-4-methylphenol unit. The energy gap between HOMO and LUMO of HL¹ is 3.626 eV. In case of deprotonated form, L¹, most of the charge density of HOMO resides on the 2,6-bis-iminomethyl-4-methylphenol and however in LUMO, it is on the same unit extended towards benzimidazole part. Here the HOMO-LUMO energy gap is 2.264 eV. The optimized structures of HL¹ and L¹

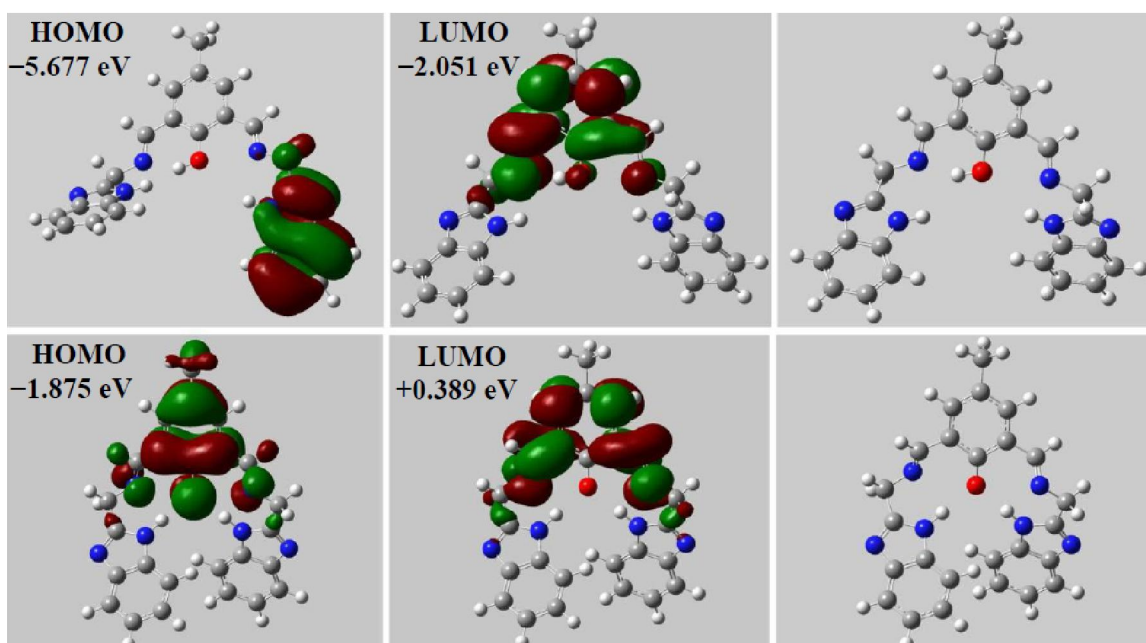


Figure 5 : Molecular orbitals plot of HL¹ (first row) and L¹ (second row), DFT optimized structures of HL¹ and L¹ were shown in the figure at the extreme right

ies of the compound are reversible with the change in pH which supports in the favor of the stability of the compound.

Density functional Theoretical (DFT) studies

To gain additional understanding of the excited state character of HL¹ and L¹, density functional theory (DFT) calculations were performed using Gaussian-09 software over a Red Hat Linux IBM cluster. Molecular level interactions between HL¹ and L¹ have been studied using DFT with the B3LYP/6-31G (d) functional model and basis set (Figure

were shown in Figure 5. The DFT calculations reveal that the energy difference between the HOMO-LUMO of HL¹ and L¹ was reduced upon the deprotonation, which may resembles with the red shift found in the UV-vis absorption measurement.

Fluorescence imaging in living cells

We applied the probe HL¹ to human cervical cancer cell, HeLa to examine whether it can work in biological systems. The extracellular pH was changed by the addition of 5mM KOH or 50mM HCl to DMEM, and the responses of intracellular pHs

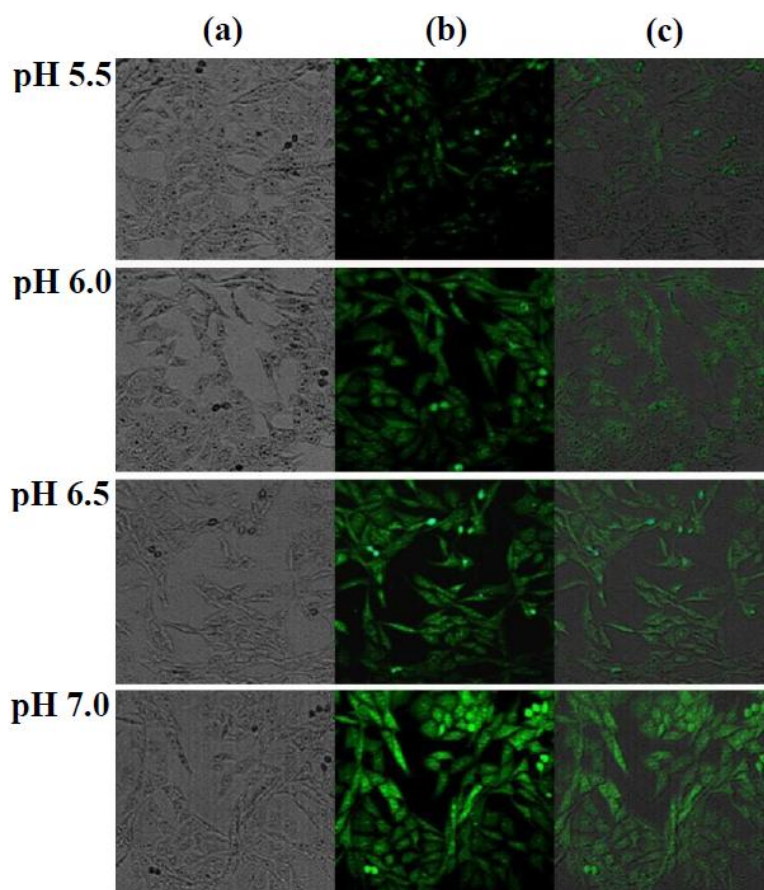


Figure 6 : Fluorescence images of HeLa cells with concomitant increase in pH (5.5, 6.0, 6.5 and 7.0) incubated with 10 μM of HL¹ for 20 min at 25 °C in DMEM. The extracellular pH was changed by the addition of 5 mM KOH or 50 mM HCl to DMEM and the responses of intracellular pHs were monitored ($\lambda_{\text{ex}} \sim 425 \text{ nm}$). (a), (b) and (c) represent the phase contrast, fluorescence and ratio of the fluorescence with the corresponding phase contrast images respectively

were monitored by fluorescence microscopy. The cells were incubated with the probe (10 μM) for 30 min at 25 °C at different pH values (5.5, 6.0, 6.5, and 7.0). The probe distribution within the cells was monitored by fluorescence microscopy following excitation at $\sim 425 \text{ nm}$ (Figure 6). The fluorescence intensities are different within the cells, which is consistent with the different intracellular distribution of H^+ ion concentration. The fluorescence ratiometric images with the corresponding phase contrast images (Figure 6) also demonstrate the different fluorescence distribution of the probe molecule inside the cells with the variation of pH. In addition to that, 10 μM of HL¹ did not show any significant cytotoxic effect (Figure 7) on HeLa for at least up to 6 h of its treatment though there was significant cytotoxicity for higher doses after 6 h onward. These results indicate that this simple,

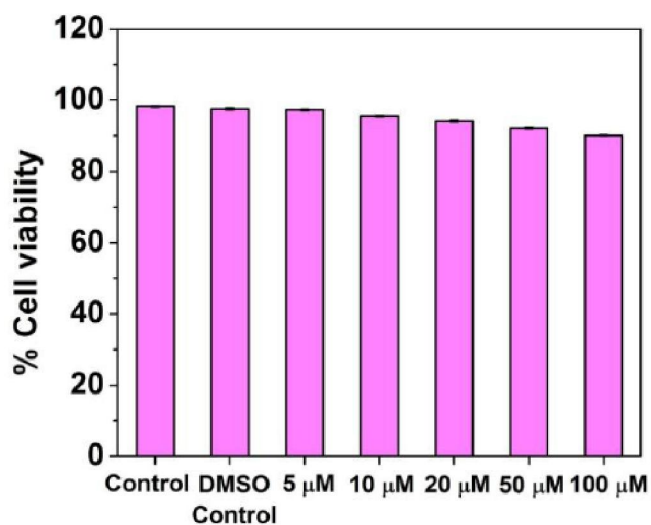


Figure 7 : Cytotoxic effect of HL¹ (5, 10, 20, 50 and 100 μM) in HeLa cells incubated for 6 h.

highly sensitive fluorescent probe, HL¹ is an efficient candidate for monitoring changes in intracel-

Full Paper

lular pH and will be of great benefit for biomedical researchers investigating the effects of H⁺ in biological systems.

CONCLUSIONS

In conclusion, a newly designed molecule, 2,6-bis-[(1-H-benzoimidazol-2-ylmethylimino)-methyl]-4-methyl-phenol (HL¹) acts as a highly selective and sensitive fluorescent pH responsive probe in a Britton-Robinson buffer at 25 °C. It shows more than 36-fold increase in the emission intensities ($\lambda_{\text{max}} = 536 \text{ nm}$) within the pH range 5.0 - 8.5 which reveals the sensitivity of the pH. The calculated p*K*_a value is 6.99 suitable for studying many of the biological organelles. This fluorescence increase with increase in pH is accounted by the formation of more fluorescent L¹ (phenoxide) ion from the less fluorescent phenolic HL¹ in higher pH. It is highly convenient for biological application as the excitation wavelengths (λ_{ex} : 425 nm) working in the visible range, and the fluorescence intensities are almost unaffected by the biologically significant (Na⁺, K⁺, Ca²⁺, Fe²⁺, Zn²⁺ etc.) and other interfering metal (Cr³⁺, Pb²⁺, Hg²⁺, etc.) ions. Also we have demonstrated the significance of HL¹ by monitoring intracellular H⁺ concentration within the human cervical cancer cell, HeLa.

ACKNOWLEDGEMENTS

Financial assistance from Department of Science and Technology (DST), New Delhi for providing Fast track research grant (vide project no. SB/FT/CS-142/2012) and University Grants Commission (UGC, vide project no. PSW-026/14-15) are gratefully acknowledged.

REFERENCES

- [1] H.N.Kim, M.H.Lee, H.J.Kim, J.S.Kim, J.Yoon; *Chem.Soc.Rev.*, **37**, 1465-1472 (2008).
- [2] E.L.Que, D.W.Domaille, C.J.Chang; *Chem.Rev.*, **108**, 1517-1549 (2008).
- [3] J.I.Peterson, G.G.Vurek; *Science*, **224**, 123-127 (1984).
- [4] J.R.Lakowicz; *Principles of fluorescence spectroscopy*, Kluwer Academic/Plenum Publishers, New York, (1999).
- [5] B.L.Feringa, *Molecular Switches*, Wiley-VCH, Weinheim, (2001).
- [6] Z.Wang, G.Zheng, P.Lu; *Org.Lett.*, **7**, 3669-3672 (2005).
- [7] R.Martínez-Zaguilán, B.F.Chinnock, S.Wald-Hopkins, M.Bernas, D.Way, M.Weinand, M.H.Witte, R.J.Gillies; *J.Cell Physiol.Biochem.*, **6**, 169-184 (1996).
- [8] H.Satoh, H.Hayashi, H.Katoh, H.Terada, A.Kobayashi; *Am.J.Physiol.Heart Circ.Physiol.*, **268**, H1239-H1248 (1995).
- [9] C.T.Okamoto; *Adv.Drug Delivery Rev.*, **29**, 215-228 (1998).
- [10] J.J.Falke, R.B.Bass, S.L.Butler, S.A.Chervitz, M.A.Danielson; *Annu.Rev.Cell Dev.Biol.*, **13**, 457-512 (1997).
- [11] H.H.Felle; *J.Exp.Bot.*, **47**, 967-973 (1996).
- [12] R.Putnam; *Intracellular pH regulation*, Academic Press, San Diego, CA., (1998).
- [13] M.S.Briggs, D.D.Burns, M.E.Cooper, S.J.Gregory; *Chem.Commun*, 2323-2324 (2000).
- [14] R.Pal, D.Parker; *Chem.Commun*, 474-476 (2007).
- [15] K.M.Sun, C.K.McLaughlin, D.R.Lantero, R.A.Manderville; *J.Am.Chem.Soc.*, **129**, 1894-1895 (2007).
- [16] J.A.Thomas, R.N.Buchsbaum, A.Zimniak, E.Racker; *BioChem.*, **18**, 2210-2218 (1979).
- [17] A.H.Lee, I.F.Tannock; *Cancer Res.*, **58**, 1901-1908 (1998).
- [18] M.A.Ramirez, R.Toriano, M.Parisi, G.Malnic; *J.Membr.Biol.*, **177**, 149-157 (2000).
- [19] H.J.Lin, P.Herman, J.S.Kang, J.R.Lakowicz; *Anal.Biochem.*, **294**, 118-125 (2001).
- [20] F.Galindo, M.I.Burguete, L.Vigara, S.V.Luis, N.Kabir, J.Gavrilovic, D.A.Russell; *Angew.Chem.Int.Ed.*, **44**, 6504-6508 (2005).
- [21] B.Tang, X.Liu, K.Xu, H.Huang, G.Yang, L.An; *Chem.Commun.*, 3726-3728 (2007).
- [22] M.H.Kim, M.J.An, J.H.Hong, B.H.Jeong, O.Kwon, J.Y.Hyon, S.C.Hong, K.J.Lee, B.R.Cho; *Angew.Chem.Int.Ed.*, **47**, 2231-2234 (2008).
- [23] J.Han, A.Loudet, R.Barhoumi, R.C.Burghardt, K.Burgess; *J.Am.Chem.Soc.*, **131**, 1642-1643 (2009).
- [24] Z.Liu, C.Zhang, W.He, F.Qian, X.Yang, X.Gao, Z.Guo; *New J.Chem.*, **34**, 656-660 (2010).
- [25] W.Zhang, B.Tang, X.Liu, Y.Liu, K.Xu, J.Ma,

- L.Tong, G.Yang; *Analyst*, **134**, 367-371 (2009).
- [26] T.Bagar, K.Altenbach, N.D.Read, M.Benčina; *Eukaryotic Cell*, **8**, 703-712 (2009).
- [27] B.Tang, F.Yu, P.Li, L.Tong, X.Duan, T.Xie, X.Wang; *J.Am.Chem.Soc.*, **131**, 3016-3023 (2009).
- [28] M.Bradley, L.Alexander, K.Duncan, M.Chennaoui, A.C.Jones, R.M.Sánchez-Martín; *Bioorg.Med.Chem.Lett.*, **18**, 313-317 (2008).
- [29] R.R.Gagne, C.L.Spiro, T.J.Smith, C.A.Hamann, W.R.Thies, A.D.Shiemke; *J.Am.Chem.Soc.*, **103**, 4073-4081 (1981).
- [30] E.Austin, M.Gouterman; *Bioinorg.Chem.*, **9**, 281-298 (1978).
- [31] H.Du, R-C.A.Fuh, J.Li, L.A.Corkan, J.S.Lindsey; *Photochemistry and Photobiology*, **68**, 141-142 (1998).
- [32] L.Henderson; *J.Am.J.Physiol.*, **21**, 173-179 (1908).
- [33] K.A.Z.Hasselbalch; *Biochemische Zeitschrift*, **78**, 112-144 (1917).
- [34] J.Ratha, K.N.Majumdar, S.K.Mandal, R.Bera, C.Sarkar, B.Saha, C.Mandal, K.D.Saha, R.Bhadra; *Mol.Cell Biochem.*, **290**, 113-123 (2006).
- [35] M.Mukhopadhyay, D.Banerjee, S.Mukherjee; *J.Phys.Chem.A*, **110**, 12743-12751 (2006).
- [36] S.Mitra, S.Mukherjee; *J.Lumin*, **118**, 1-11 (2006).